International Biodeterioration & Biodegradation 203 (2025) 106128

Contents lists available at ScienceDirect

International Biodeterioration & Biodegradation

journal homepage: www.elsevier.com/locate/ibiod

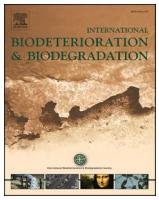

Essential oils in hydrogel for microalgal biofilm removal: Application strategies for stone heritage preservation

Roberta Ranaldi [a,1], Francesco Gabriele [b,*], Lorenza Rugnini [a], Patrick Di Martino [c], Rémy Agniel [c], Francesco Scuderi [a], Roberto Braglia [a], Antonella Canini [a], Nicoletta Spreti [b]

[a] Department of Biology, Tor Vergata University of Rome, Via della Ricerca Scientifica 1, 00133, Rome, Italy
[b] Department of Physical and Chemical Sciences, University of L'Aquila, Via Vetoio, Coppito, I-67100, L'Aquila, Italy
[c] ERRMECe Laboratory, University of Cergy-Paris, rue 13 Descartes site de Neuville-sur-Oise, 95031, Cergy-Pontoise, France

ARTICLE INFO

Keywords:
Colosseum hypogeum
Biodeteriogens
Microalgal biofilm
Green biocides
Essential oils
Hydrogel

ABSTRACT

This study faces the critical need to develop new eco-friendly biocides and effective application strategies to mitigate phototrophic biodeteriogens in cultural heritage sites. To address this challenge, a microalgal strain previously collected from the hypogeum of the Colosseum (Rome, Italy) was used to induce biofilm formation on Lecce stone specimens. The samples were treated with 0.5% and 1% of essential oils (EOs) from *Thymus vulgaris* L., *Origanum vulgare* L. and *Cinnamomum verum* Presl. The EOs were encapsulated in an alginate hydrogel support matrix (HG) and applied to the biofilms with different application times (24 h and 48 h). A mini-PAM portable fluorometer was used to determine the phototrophic activity up to 2 months after treatment. Scanning electron microscopy was used to investigate the effects of EOs on microalgal cell morphology within biofilms, while Fourier transform infrared spectroscopy analyzed changes in biomolecular distribution after treatment. The findings revealed that all EOs were effective when encapsulated in HG. However, by the end of the monitoring period, only cinnamon EO maintained photosynthetic inhibition, especially when applied at 0.5% for 48 h. Moreover, biofilm treated with cinnamon EO showed the most significant effects, particularly in disrupting cell membranes and reducing lipids signals, ultimately leading to cell lysis. This approach effectively inhibited the vitality of biofilm-forming phototrophs on stone surfaces, using low concentrations of EO for defined periods of time.

1. Introduction

In recent years, the role of scientists in protecting cultural heritage from biofilm inducing deterioration has gained increasing significance. This effort necessitates an interdisciplinary approach, integrating different scientific fields to enhance our understanding and develop effective conservation strategies. A crucial aspect of this process is fostering dialogue with restorers to address their practical needs, particularly concerning the application of biocides. In fact, effective conservation must not only prioritize the eradication of biodeteriogenic biofilm but also ensure that restoration interventions remain as minimally invasive as possible. Striking this careful balance is essential to preserve the historical and artistic integrity of cultural assets while minimizing restoration activities (Avdanina and Zhgun, 2024). One of the major challenges in this context is to distinguish the biodeteriorative, neutral, or even protective roles of biofilms, due to their intricate interactions with the substrate and the surrounding atmospheric ecosystem (Berti et al., 2024). This complexity makes it imperative to conduct thorough investigations before implementing restoration measures. However, despite the critical importance of understanding biofilm characteristics, such analyses are often prohibitively expensive and time-consuming. Furthermore, the dynamic nature of these microbial communities, which can evolve or mutate in response to environmental changes, leads to the development of tolerance and resistance to biocidal treatments or to the acquision of new functional capacities (Sanmartín et al., 2023). This underscores the need for sustainable and adaptive conservation strategies that consider the resilience and adaptability of these microorganisms.

Biofilm growth is strongly influenced by abiotic factors, such as water availability, which is a fundamental prerequisite. Once formed,

* Corresponding author.
E-mail address: francesco.gabriele@univaq.it (F. Gabriele).
[1] PhD program in Evolutionary Biology and Ecology, Department of Biology, Tor Vergata University of Rome, Via della Ricerca Scientifica 1, 00133 Rome, Italy.

https://doi.org/10.1016/j.ibiod.2025.106128
Received 24 March 2025; Accepted 18 May 2025
Available online 24 May 2025

they can retain water on the stone, thereby increasing the water vapor uptake, which is associated with biodeterioration processes (Wang et al., 2025). Another crucial factor is the presence of light, both natural and artificial, which facilitates the proliferation of phototrophic microorganisms. Therefore, controlling lighting conditions can be an effective strategy to mitigate the biodeterioration of cultural assets (Méndez et al., 2024). Nevertheless, as reported by Rugnini et al. (2020), phototrophic microorganisms can grow also in quasi-darkness conditions, as in the case of Domus Aurea (Rome, Italy). The ability of microorganisms to tolerate a broad range of environmental conditions means that under optimal circumstances they can proliferate rapidly (Stanaszek-Tomal, 2020), potentially causing damage to valuable materials. Beyond structural degradation, biodeteriogenic microorganisms, both phototrophic and heterotrophic, can also alter the aesthetic appearance of the substrate by inducing discoloration, surface covering, or secretion of diffusible pigmentation (Avdanina and Zhgun, 2024), thereby affecting public visitors' perception of the value of cultural assets. For example, in the catacombs of SS. Marcellino and Pietro (Rome, Italy), fungal colonization has compromised not only the visitor experience but also the overall conservation state of the monument (De Leo et al., 2022). More critically, their pigmented biofilms often cause structural damage through hyphal invasion or mineral extraction from stone substrates (Liu et al., 2020). Traditionally, the control of these microorganisms has relied on disinfectants containing quaternary ammonium salts. Although these agents have been extensively studied in terms of safety, eco-toxicity and their role in promoting biological resistance is now well-known (Paolino et al., 2024), growing concerns about their environmental impact have driven the search for more sustainable and greener solutions.

Plant extracts such as essential oils (EOs) have emerged as promising alternatives, due to their broad-spectrum antimicrobial properties (de Sousa et al., 2023). Their potential application in cultural heritage conservation has also been increasingly explored (Cirone et al., 2023; Russo and Palla, 2023; Reale et al., 2024), with various mechanisms of action proposed for their effects on bacteria and fungi (Hou et al., 2022). However, their impact on microalgae remains poorly understood and even less well-documented. Additionally, standardized protocols for their application in cultural heritage preservation are still lacking (Gu, 2024). Encapsulation of EOs in hydrogel matrices (HG) is a promising technique currently used in a wide range of applications, from biomedicine to the food industry (Chelu, 2024). Even in the field of cultural heritage conservation, many of the drawbacks of using active compounds in solution can be overcome with this approach. By incorporating them into inert matrices, it is possible to reduce both the amount of product required for cleaning and the penetration and diffusion of the solvent on the artwork along with the easy removal of microorganisms and by-products from its surface (Baglioni et al., 2014; Chelazzi et al., 2018). This method overcomes many of the limitations associated with conventional treatments and offers a more controlled and effective application.

Hence, in this study, we aim to investigate the efficacy of EOs and their effect on phototrophic cells, particularly biofilm-forming microalgae, which are widespread in both hypogean environment and open-air cultural heritage sites. Furthermore, we seek to define optimal application parameters in terms of EOs concentration and timing of application to overcome the challenges of developing green and sustainable conservation solutions. By addressing these key aspects, this research aimed to design an application protocol tailored to the practical needs of restorers, ensuring both efficacy and ease of use in the field.

2. Materials and methods

2.1. Stone colonization

In this study, an artificial biofilm was created using a microalgal strain belonging to the order of Chlorellales, previously enriched from biofilms sampled in the Colosseum hypogeum (Ranaldi et al., 2025). Lecce stone samples (5 × 5 × 2 cm; sourced from DÉCOR, Monteroni, LE, Italy) had been autoclaved at 121 °C for 20 min, and then the biomass (1 mL) was evenly spread over the surface. All stones were placed on sheets of filter paper inside transparent plastic boxes with lid, which were perforated to allow air flow (Gabriele et al., 2023). Firstly, 30 mL of dH_2O was applied to the underside of each box and then was constantly added to maintain a high degree of stone hydration (90% RH). Biofilms were sprayed once a week for six months with BG11 culture medium (Rippka et al., 1979) to promote cells growth and kept in controlled culture conditions (22 ± 2 °C; 10 μmol photons m^{-2} s^{-1}; 12 h light/dark of photoperiod).

2.2. Preparation and application of biocide hydrogel system

The EOs of *Thymus vulgaris* L. (**T**), *Origanum vulgare* L. (**O**) and *Cinnamomum verum* Presl. (**C**), (L'Aromoteca S. a.S. - Assago, Milan, Italy) were tested against the microalgal biofilm enriched from the Colosseum hypogeum. Each oil was individually included at 0.5% and 1% concentration with 5% wt. alginate and 0.2% wt. $CaCl_2$, prepared by suspending low viscosity sodium alginate (Sigma-Aldrich) in dH_2O and under vigorous mechanical stirring at room temperature to the homogeneous polysaccharide dispersion and then a calcium chloride solution was slowly added. 200 mg of EO-HG formulations were applied to Japanese paper (20 μm thickness, 6 g/m^2 fiber density) placed on the biofilm above the stone surfaces and after 24 h, the dried hydrogel-biocide system was carefully removed (Gabriele et al., 2023). The application of the same EOs at 0.5% in HG was also tested over a longer period of 48 h. For both tests, the positive control was treated with the antimicrobial BIOBAN™ 104 (CTRL + B) (Dow Chemical Company, Michigan, USA), a commercial product composed of a mixture of octylisothiazolinone and quaternary ammonium compound. The liquid solution was diluted at 3% (v/v) and applied by pipetting it on biofilm. Two stone samples were used as negative controls: one treated with pure HG (CTRL - HG) and the other was untreated (CTRL -).

2.3. Measurement of the photosynthetic activity

For all the experimental set-up, the effect of EOs-HG system on biofilms growth on Lecce stone fragments was evaluated by measuring the chlorophyll fluorescence of phototrophs with a portable pulse amplitude fluorometer (Mini-PAM) (Walz GmbH, Effeltrich, Germany) combined with WinControl software. The photosynthetic activity reported as yield (F_m - F_0/F_m) were obtained in a quasi-darkness room and each sample was dark adapted for 30 min before each measurement. A probe equipped with a holder that holds the fiber at a distance of 6 mm and at an angle of 60° from the biofilm on stone surfaces was used for the analyses (Rugnini et al., 2020). The biocidal effect of EOs on biofilms was monitored before each treatment (t_0), soon after hydrogel removal (t_s) and after 1 week (t_{1w}), 2 weeks (t_{2w}), 1 month (t_{1m}) and 2 months (t_{2m}). For each stone, the measurements of photosynthetic activity were recorded at 25 different points obtained with a detachable grid. Until the end of the experiments, each stone was kept under controlled growth conditions (T = 22 ± 2 °C; irradiance = 10 μmol photons m^2/s^{-1}; photoperiod: 12 h light/dark).

2.4. Microscopy observation

Scanning Electron Microscopy (SEM) was employed to observe the morphological alteration of the cells forming biofilm on the stones after the treatment with 1% EOs encapsulated in HG, compared to the controls. To preserve the integrity of the biofilms, which were subsequently analyzed by Fourier Transform Infrared Spectroscopy (FTIR), the samples were not metallized. Before the SEM investigation, all samples underwent a dehydration process by immersion in ethanol at gradually increasing concentrations: 30% × 10 min; 50% × 10 min; 80% × 10

min; 100%, 2 × 10 min. Then, all stone samples were covered with aluminum foil and stored in an oven (HB-1000 Hybridizer, UVP Laboratory products) for at least 2 days at 50 °C. SEM analysis was performed using ZEISS GeminiSEM 300 equipped with a VPSE detector, set in low vacuum mode at about 30 Pa, operating at a working distance of 9.0 mm and an accelerating voltage of 7 kV. Due to the inhomogeneous biopatina, two photos were acquired for five areas of each sample (N = 10).

2.5. FTIR analysis

After SEM observations, the dried biofilms treated with 1% EO-HG were scraped from the surface with a sterile scalpel and homogenized before analysis by Fourier-transform infrared spectroscopy (FTIR) (ALPHA-P, BRUKER). Analyses were performed with 32 accumulations per sample from 500 cm^{-1} to 4000 cm^{-1} with a resolution of 2 cm^{-1}. Six measurements were taken for each sample using the OPUS 8.5 (SP1) program. A minimum-maximum normalization of the spectra was carried out.

2.6. Statistical analysis

GraphPad Prism 10.2.3 software was used to perform the statistical analysis and to generate the plots. The data obtained from the PAM measurements were analyzed using the parametric test ordinary one-way ANOVA, comparing the groups with each other. Different letters indicate significant differences ($p < 0.05$) in the statistical analysis. The unpaired *t*-test was used for the FTIR data to compare each sample with the negative control (CTRL -). P values were considered significant, very significant, highly significant and extremely significant when they were less than 0.05, 0.01, 0.001 and 0.0001. The significance was represented as *, **, *** and ****, respectively. All reported results are expressed as mean ± SD (standard deviation).

3. Results and discussion

3.1. Effect of EOs-HG on microalgal biofilm photosynthesis

This study investigates the effect of thyme, oregano and cinnamon EOs (**T**, **O** and **C**, respectively) at two concentrations (0.5% and 1%) suspended in an alginate hydrogel matrix, and applied on microalgal biofilms for 24 h. The compositional profiles of the three EOs were previously reported (Ranaldi et al., 2025). Briefly, **T** and **O** consist mainly of thymol and carvacrol, respectively, followed by *p*-cymene and γ-terpinene, while the most abundant component in **C** is (*E*)-cinnamaldehyde (more than 70%). The results of photosynthetic yield over time are shown in Fig. 1.

As can be seen in Fig. 1, the untreated biofilms (CTRL -) remain stable over time, with values ranging from 0.663 ± 0.026 (t_0) to 0.591 ± 0.019 (t_{2m}). The same situation was observed for the biofilm treated with pure HG (CTRL - HG), confirming that the hydrogel without any biocide inside did not induce any alteration in the microalgal biofilm. Conversely, the positive control treated with BIOBAN™ 104 (CTRL + B) reduced the photosynthetic yield value by 86% after 24 h of application, corresponding to the removal of the hydrogel for the other stones (t_s). However, the value gradually increased over time during the monitoring period and reached 0.563 ± 0.039 two months after the treatment (t_{2m}).

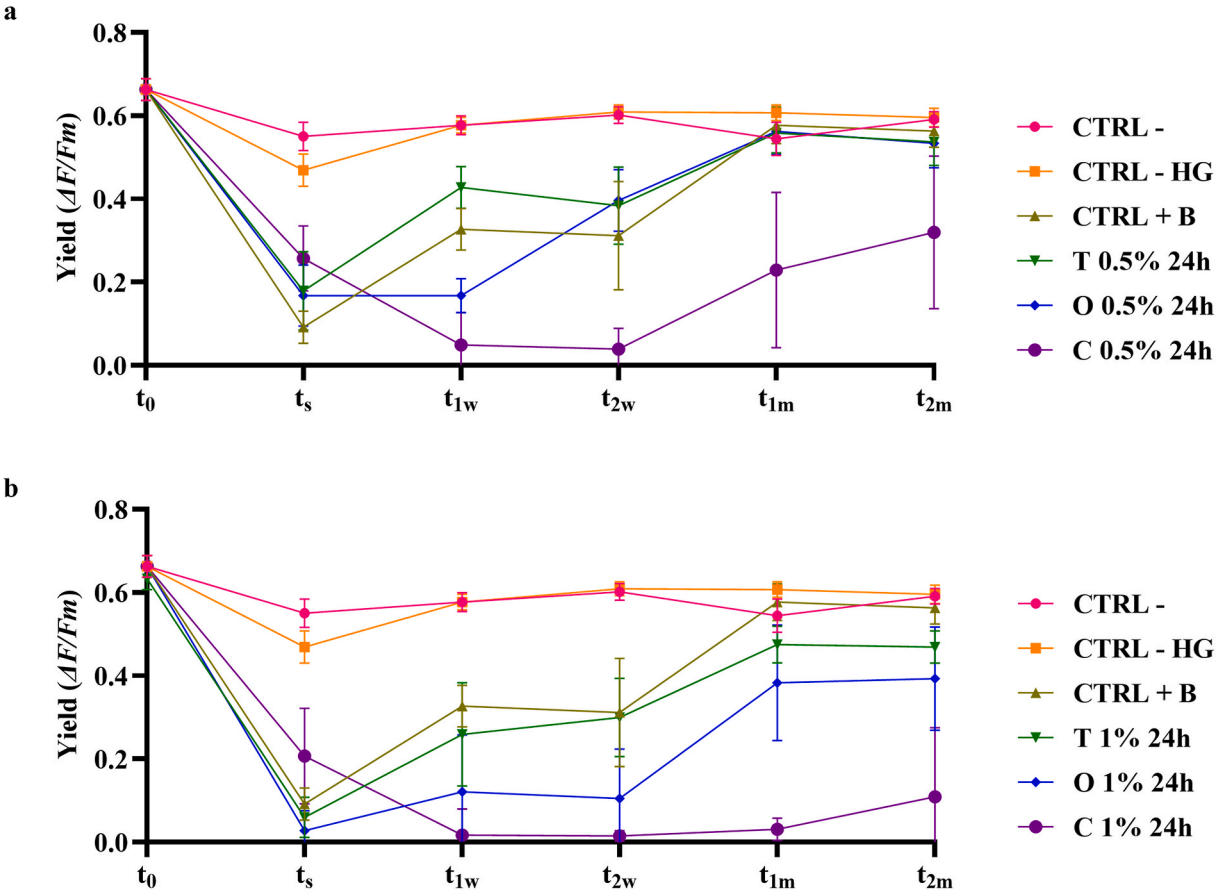

Fig. 1. Photosynthetic yield of biofilms grown on untreated stones (CTRL -), stones treated with pure hydrogel (CTRL - HG) and with BIOBAN™ 104 (CTRL + B). The EOs of thyme (**T**), oregano (**O**) and cinnamon (**C**) were tested a) at 0.5% and b) 1% for 24 h. The plot illustrates the yield trends over time: t_0 (before treatment), t_s (immediately after hydrogel removal), t_{1w} (one week post-treatment), t_{2w} (two weeks post-treatment), t_{1m} (one month post-treatment), and t_{2m} (two months post-treatment). Data represent means ± SD (N = 25).

T, **O** and **C** applied at 0.5% and 1% for 24 h (Fig. 1a and b, respectively) showed their effectiveness in strongly decreasing the photosynthetic activity of biofilms just after treatment. In particular, immediately after HG removal (t_s), **T** and **O** at 0.5 and 1% reduced the yield values by about 70% and more than 90%, respectively. On the other hand, a decrease of about 60% was observed for **C**-treated samples, regardless of the concentration of EO. Differently from this work, in which thyme EO was tested against green microalgae biofilm, Ranaldi et al. (2022) demonstrated the complete effectiveness of 0.5% *T. vulgaris* EO encapsulated in alginate hydrogel when applied for 24 h to various cyanobacterial strains cultivated on agar plates, reducing photosynthesis to zero after hydrogel removal. Similarly, Gabriele et al. (2023) reported successful application of *T. vulgaris* EO (0.1% and 0.25%) and its main active compound, thymol (0.07% and 0.18%), in alginate hydrogel against cyanobacterial strains cultivated on stones. Thymol, the main component of thyme EO, incorporated in a waterborne paint at 2% w/w, exhibited algaecide activity and its effectiveness in inhibiting the growth of phototropic organisms was mainly attributed to its action on the cytoplasmic membrane, causing its structural disorganization, which affects cell permeability (Gómez de Saravia et al., 2018). The good activity of the EO from *Thymbra capitata* against green microalgae and cyanobacteria has also been attributed to its interaction with the cell membrane that causes the alteration of the lipid bilayer. Carvacrol, the principal component, together with *p*-cymene and γ-terpinene, were the main contributors to its antimicrobial activity (Gagliano Candela et al., 2019). Oregano EO and eugenol were recently employed by Bartoli et al. (2024) against green microalgae and filamentous cyanobacteria collected from the Aurelian Walls in Rome. The tests using silica nanocapsules containing either 1 or 3 mg of the substance showed a decrease in fluorescence under UV light, indicating a reduction in microbial vitality and colonization. These results strongly suggest that thyme and oregano EOs exhibit a higher effectiveness against cyanobacterial biofilms compared to the green microalgae studied here, underscoring the potential to develop a species-specific targeted biocide. For example, in Argyri et al. (2021) 18 EOs were tested and, among them, *O. vulgare* EO at 0.1% was the most effective, inhibiting the growth of all fungi and bacteria isolated from Petralona Cave (Halkidiki, Greece).

The effectiveness of three EOs (from *Origanum vulgare*, *Thymus vulgaris* and *Calamintha nepeta*) and their main components, embedded into a PVA gellan-based hydrogel, was tested under laboratory conditions (Genova et al., 2020) and *in situ* on an outdoor granite wall in Santiago de Compostela (Genova et al., 2023) against phototrophic biofilms, mainly composed of cyanobacteria and algae, growing on granite buildings. The treatments were allowed to act for one week when applied in the laboratory, and *C. nepeta* proved to be the most effective. In the *in situ* experiments, the application was extended to one month, and in this case, the best results were obtained with the oregano EO due to the high percentage of carvacrol, the main factor responsible for its biocidal activities.

Differently from thyme and oregano EOs, where the minimum value of photosynthetic yield was measured soon after the removal of the treatment (t_s), cinnamon EO exhibited a gradual decrease in yield at both concentrations tested, reaching 94% and 97% at 0.5% and 1% concentrations, respectively, two weeks after application (t_{2w}) (Fig. 1). However, after two months (t_{2m}), a partial recovery of the photosynthetic yield was observed, but still lower than that of **T-** and **O**-treated samples. Its highest biocidal activity has been confirmed in the literature by numerous investigations in medical, veterinary, cosmetic and food applications (Nabavi et al., 2015; Dutta and Chakraborty, 2018; Chen et al., 2024). The antimicrobial and antifungal properties have recently been studied also in the field of cultural heritage, by evaluating the effectiveness of cinnamon extracts, either applied as an aqueous solution using the agar diffusion method (Lee and Chung, 2023) or by spraying it dissolved in *Citrus aurantium* var. *amara* hydrolate (Di Vito et al., 2022). Moreover, in Minotti et al. (2022), this last green antimicrobial emulsion was preliminary applied by spraying on canvas samples (*in vitro* test) and then *in situ* on the canvas "Il Silenzio" by Jacopo Zucchi of the Uffizi Museum (Florence, Italy), showing good antifungal activity in both cases. It has also been reported that the efficacy of *Cinnamomum cassia* EO in inhibiting the growth of algae and mosses from stone surfaces (Long et al., 2024) is related to its high cinnamaldehyde content, due to its ability to alter the composition of cell membranes, and when incorporated into commercial silicone coatings it was able to inhibit the formation of phototrophic biofilms on stone surfaces (Cuzman et al., 2011).

In order to maximize the effectiveness of the EOs using the lowest biocide concentration, the biocide exposure time was extended to 48 h (Fig. 2).

As shown in Fig. 2, shortly after the removal of the hydrogel (t_s), the photosynthetic activity has almost completely disappeared, regardless of the encapsulated EO. However, samples treated with **T** and **O**, after two months, showed values of photosynthetic yield higher than 0.4, despite their different rate of recovery. On the other hand, **C** applied for 48 h, was the only treatment in which the yield value decreased close to zero from the removal of the support matrix (t_s) to the end of the monitoring period (t_{2m}). Even the positive control, BIOBAN™ 104, after 48 h from the treatment (t_s) leads to a progressive re-increase in photosynthetic yield until a complete restoration after two months. Therefore, this study suggests that extending the application time enhances the effectiveness of the treatment by prolonging its effects on the biofilm over time.

Similarly, the EO from *Cinnamon zeylanicum* (bark) was effective against a natural biofilm composed of a mixture of microorganisms, including green unicellular algae colonizing a marble slab (Spada et al., 2021). In fact, its encapsulation in agar-agar water solution at 0.75% (w/w), or as a mixture with other EOs, and its application as a poultice for 10 days at (~37 °C), allowed to reduce the ATP values of the biofilm. In our experimental condition, a lower EO concentration (0.5%) and a shorter treatment duration (48 h) achieved comparable results.

As show in Table S1 (see supplementary material), the comparison among all tested treatments suggests that the negative control treated with pure HG (CTRL - HG) was statistically different from the untreated sample (CTRL -) only immediately after HG removal, likely due to the peel-off effect of the technique. However, no differences were observed for the rest of the experiment, highlighting that pure HG did not exhibit a biocidal effect against microalgae and could therefore be considered an inert matrix. In contrast, the positive control BIOBAN™ 104 (CTRL + B) remained statistically different from the two negative controls for up to two weeks after treatment. This reflects the scenario occurring in the hypogeum of Colosseum, where the resistance to conventional biocides of a complex biofilm led to more frequent disinfections of floorings in conjunction with water washing (Ranaldi et al., 2025).

Among the green biocides tested in this work, **T** and **O** were effective at both 1% for 24 h and 0.5% for 48 h, showing a significant difference from the two negative controls up to two months after application. At the end of the experiment (t_{2m}), using **T** or **O**, there were no statistical differences between the application at 1% for 24 h and 0.5% for 48 h; however, in both cases, the photosynthetic activity levels remained too high to be considered a viable replacement for traditional biocides. In contrast, **C** effectively reduced photosynthetic activity to almost zero by two weeks, showing no differences in terms of concentrations and application times tested. Moreover, at t_{2m}, samples treated with **C** showed the most pronounced effect when applied at 0.5% for 48 h. This result was statistically different from the applications at 1% and 0.5% for 24 h, as well as from the negative controls. This suggests that **C** exhibits a longer lasting biocidal efficacy over time even at low concentration. Therefore, these results recommend that **C** at 0.5% for 48 h could be a valuable and sustainable alternative to traditional chemical biocides for controlling the growth of microalgal biofilms on stone cultural heritage.

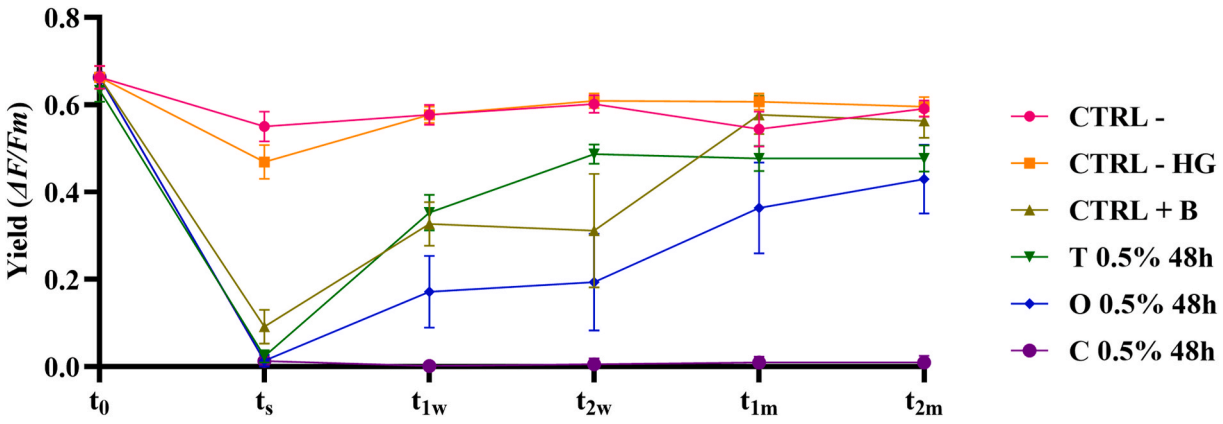

Fig. 2. Photosynthetic yield of biofilms grown untreated stones (CTRL -), stones treated with pure hydrogel (CTRL - HG) and with BIOBAN™ 104 (CTRL + B). The EOs of thyme (T), oregano (O) and cinnamon (C) were tested at 0.5% for 48 h. The plot illustrates the yield trends over time: t_0 (before treatment), t_s (immediately after hydrogel removal), t_{1w} (one week post-treatment), t_{2w} (two weeks post-treatment), t_{1m} (one month post-treatment), and t_{2m} (two months post-treatment). Data represent means ± SD (N = 25).

3.2. Investigation of the influence of EOs on cell morphology

The effects of biocidal treatments on microalgal cells within biofilms grown on Lecce stones were evaluated by SEM. Although the biocidal activity of EOs is well established, their mechanisms of action are not fully understood, especially against microalgae. Investigating the effects of EOs on cell morphology can provide valuable insight into their potential mode of action (de Sousa et al., 2023). Here, SEM images were acquired two months after treatment at 1900 × magnification of the negative control (CTRL -) and samples treated with pure hydrogel (CTRL - HG), BIOBAN™ 104 (CTRL + B), thyme, oregano and cinnamon EOs at 1% concentration (Fig. 3).

The untreated biofilm (CTRL -; Fig. 3a) consisted of perfectly spherical intact cells (5 μm in diameter), wrinkled cells with a morphology similar to the microalgal biofilm of the pure HG-treated sample (Fig. 3b). Observations confirmed that this approach does not alter microalgal structure and vitality, except for a slight mechanical shrinkage effect observed after the application of the gel. Conversely, the images of the samples treated with the biocides reveal drastic changes in the appearance of the algae. Cells treated with the positive control BIOBAN™ 104 (CTRL + B; Fig. 3c) appeared 'doughnut-shaped' with a slight central depression and totally destroyed in some scattered areas of the biofilm. In fact, according to the literature, quaternary ammonium salts disrupt electrostatic membrane interactions, leading to permeabilization and lysis, or inhibit specific membrane processes such as solute transport and cell wall biosynthesis (Zhang et al., 2025). SEM images of bacterial strains treated with a novel oxadiazole-based quaternary ammonium salt solution showed extensive membrane collapse associated with the release of cytoplasm to the outside (Xie et al., 2018). However, their use can also promote biofilm formation and induce oxidative stress, which increases genetic variation and may contribute to microbial resistance (Romani et al., 2022; Sanmartín et al., 2023).

Observation of samples treated with **T** and **O** showed the coexistence of open, collapsed and slightly altered concave morphology cells (Fig. 3d and e). This inhomogeneous biopatina aligns with PAM measurements (Figs. 1 and 2), which indicate that the biofilm gradually regains vitality in certain areas, while photosynthesis inhibition persists in others. Differently, the biofilm treated with **C** (Fig. 3f) showed the most drastic morphological changes. The cells were massively lysed, opened and severely deformed, probably due to rupture of the cell membrane. The effect of different EOs on cell morphology was confirmed by Permadi et al. (2024), who used SEM to show that *Citrus aurantifolia* EO induced irregularities and shrinkage in pathogenic microorganisms associated with *Musa* spp. and that these effects became more pronounced with increasing concentration and exposure time. Other studies have focused on the effects of primary components, such as eugenol, present in the EO of cinnamon and cloves. The effect of this terpene on cell morphology of the cyanobacterium *Microcystis aeruginosa* was evaluated using transmission electron microscopy, which revealed cell rupture and membrane deformation leading to the release of extracellular organic matter. However, given the large number of components of EO and the many factors that influence their chemical composition (such as plant species, cultivation conditions and extraction processes), it is not suitable to propose a single mechanism of action (Andrade-Ochoa et al., 2021).

SEM observations revealed the persistence of necrotic biomass on stone surfaces after biocidal treatment, highlighting the need to focus future research on combining the EO-HG system with mechanical brushing to completely remove necrotic biological layers and mitigate rapid recolonization driven by secondary ecological succession. In fact, microorganisms can exploit dead biomass and biocide residues as nutrient sources for the recolonization process (Sanmartín et al., 2023). However, determining the appropriate cleaning procedure is crucial, as improper techniques can negatively impact both the quality of materials and the microbial communities, further contributing to surface contamination (Bontemps et al., 2024).

3.3. FTIR analysis

FTIR analysis of biological samples can provide valuable insights into the effects of treatments on biological patinas (Xin et al., 2017; Xiong et al., 2019). However, interpreting the spectra is highly complex due to the abundance of biomolecules and their functional groups present in such matrices.

Fig. 4 shows the mean FTIR spectra of the biopatina collected from the six samples and, to facilitate their comparison, the maximum intensity of each spectrum was normalized to unity.

The FTIR spectra highlighted the presence of the typical vibrational modes of many functional groups associated with various biomolecules, including carbohydrates, proteins, lipids, and nucleic acids (Beć et al., 2020). The vibrational frequencies of the most characteristic groups are listed in Table 1.

As evident from each spectrum, the stretching vibrations of both O-H and N-H groups associated with carbohydrates and proteins, respectively, produce a single broad absorption band, making these vibrational modes indistinguishable. The symmetrical and the anti-symmetrical C-H stretching vibrations, the C=O stretching vibrations at ~1740 cm^{-1} and the C-H bending vibrations at ~1400 cm^{-1} are attributed to the lipid fraction of the biopatina. Although these functional groups can be found in all the biomolecules, lipids contain a higher number of methyl, methylene and ester carbonyl groups. On the contrary, the stretching of

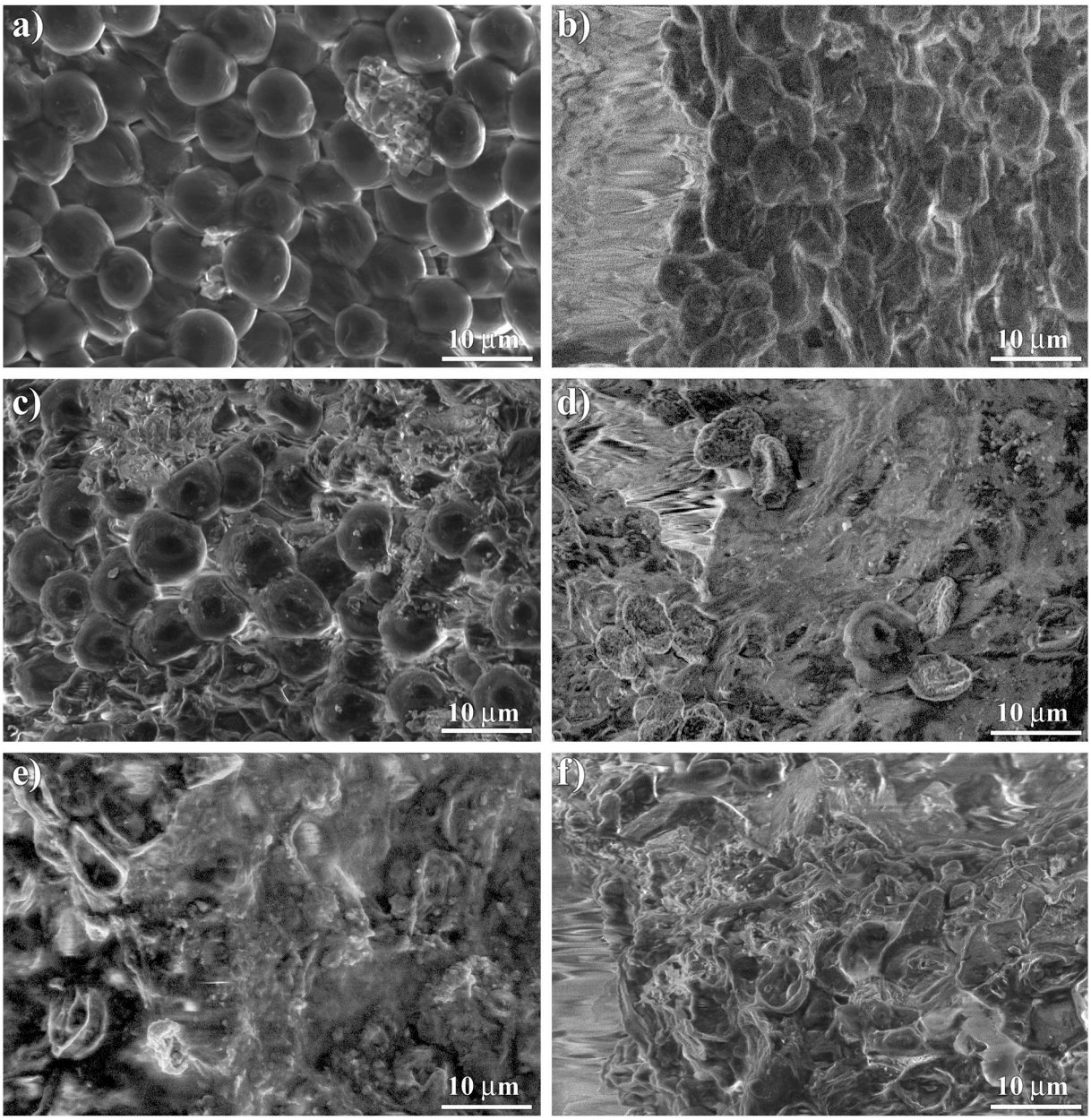

Fig. 3. SEM images of a) untreated (CTRL -) and biofilm treated with b) pure hydrogel (CTRL - HG), c) BIOBAN™ 104 (CTRL + B), d) *T. vulgaris*, e) *O. vulgare* and f) *C. verum* EOs encapsulated in alginate hydrogel. Bar = 10 µm.

the amide carbonyl group of proteins occurs at a lower frequency (~1640 cm^{-1}) and is generally identified as "Amide I" absorption band. This vibrational mode is often combined with the stretching of the C-N bonds and the bending of N-H bonds at about 1520 cm^{-1} in the amides constituting the peptide linkage, which is known as the "Amide II" absorption band.

Since phosphate groups are widely distributed in both phospholipids and nucleic acids, the anti-symmetrical stretching of the P=O bond (~1240 cm^{-1}) could provide valuable information on the distribution of these biomolecules within cells.

Lastly, the polysaccharide fraction is generally identified by characteristic absorption bands in the fingerprint region around 1000 cm^{-1} corresponding to the stretching vibrations of the C-O bonds and the skeletal vibrations of the saccharide rings.

In all the regions described, the FTIR spectra of both the negative control and the sample treated with the pure hydrogel resulted very similar, confirming that HG did not affect the biopatina. Conversely, major differences were observed when comparing the samples treated with the biocides with the untreated reference one. However, variations in the absolute absorbance values of the aforementioned bands could be misleading without an internal standard. Therefore, to better rationalize the information derived from the FTIR spectra, different ratios between the most characteristic vibrational modes were analyzed. Table 2 reports the ratios corresponding to the signal of proteins relative to lipids (A_{1640}/A_{1740}), carbohydrates signal to lipids (A_{1020}/A_{1740}) or to proteins (A_{1020}/A_{1640}) and the signal of phosphorylated compounds relative to lipids (A_{1240}/A_{1740}).

The results confirmed previous observations, highlighting no differences between the untreated and pure hydrogel-treated patinas, while revealing differences observed among the treatments applied. BIOBAN™ 104, used as a positive control, induced a significant increase in terms of proteins and phosphorylated compounds relative to lipids, nearly doubling the values observed in negative control. Additionally, it led to an approximately 60% increase in carbohydrates to lipids ratio.

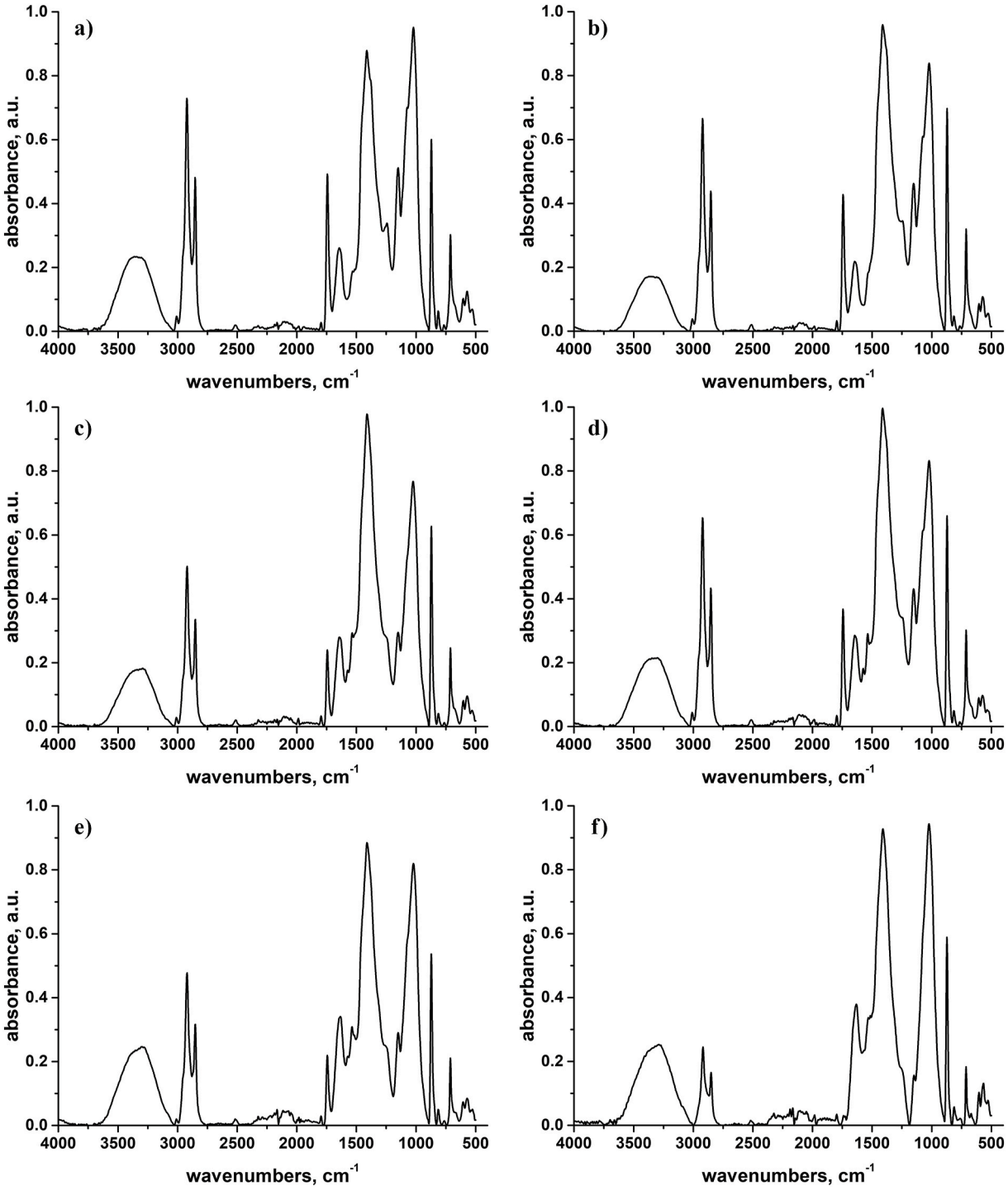

Fig. 4. FTIR spectra of a) control biofilm, those treated with b) pure hydrogel, c) BIOBAN™ 104 and with 1% of d) *T. vulgaris*, e) *O. vulgare* and f) *C. verum* EOs encapsulated in alginate hydrogel.

The treatments with **T** and **O** also resulted in significant increases in most of these ratios compared to the negative control, despite **O** exhibiting a more pronounced effect.

In comparison to the negative control, significant changes were also observed after the treatment with **C**. In fact, the ratio of proteins and carbohydrates relative to lipids was about 20 times higher than those in the reference, while the increment in the ratio of phosphorylated compounds to lipids was about one order of magnitude. As also evidenced by the SEM analysis, this may be due to the disruption of the cell membrane and the resulting leakage of intracellular organelles and cytoplasmic biomolecules, whose IR signals are partially shielded by the cell wall and membrane in the reference sample.

By combining information obtained through SEM microscopy and FTIR analysis, important insights were gained into the effects of biocides on algae grown on Lecce stone samples. BIOBAN™ 104 did not cause massive cell lysis, allowing the algae to potentially regain vitality after treatment. Likewise, thyme and oregano EOs induced notable morphological changes without significantly affecting the cell membranes of the algae. The similar effects observed in samples treated with these two EOs may be due to the analogy in their composition. Specifically, carvacrol,

Table 1
Characteristic absorption bands extrapolated by the mean FTIR spectra acquired on the biofilm grown on the six samples of Lecce stones.

Wavenumber, cm^{-1}	Assignment	Biomolecules
3200–3400	ν_s (N-H), ν_s (O-H)	carbohydrates and proteins
2800–3000	ν_s and ν_{as} (C-H) of CH_2 and CH_3	lipids
~1740	ν C=O	lipids (ester group)
~1640	ν C=O, Amide I	proteins
~1520	δ N-H, ν (C-N), Amide II	proteins
~1400	δ C-H of CH_2 and CH_3	lipids
~1240	ν_{as} (P=O)	nucleic acids and phospholipids
~1150	ν_{as} C-O-C bridge and C-O-H	carbohydrates
~1020	skeletal vibration and ν C-O	carbohydrates

Table 2
Proteins relative to lipids (A1640/A1740), carbohydrates relative to lipids (A1020/A1740) or proteins (A1020/A1640), and phosphorylated compounds relative to lipids (A1240/A1740) are expressed as mean ratios relative to the untreated control biofilm. Samples were treated with pure hydrogel, BIOBAN™ 104, or 1% of *Thymus vulgaris* (d), *Origanum vulgare* (e), and *Cinnamomum verum* (f) essential oils (EOs) encapsulated in alginate hydrogel. An unpaired *t*-test was used to compare each treatment with the negative control (CTRL -). ^{ns} not significant, *$p < 0.05$, **$p < 0.01$, ***$p < 0.001$, ****$p < 0.0001$.

	proteins/ lipids	carbohydrates/ lipids	carbohydrates/ proteins	P=O compounds/ lipids
CTRL -	0.531 ± 0.069	1.955 ± 0.219	3.718 ± 0.530	0.695 ± 0.152
CTRL - HG	0.504 ± 0.046^{ns}	2.005 ± 0.254^{ns}	4.007 ± 0.657^{ns}	0.859 ± 0.248^{ns}
CTRL + B	1.157 ± 0.165****	3.201 ± 0.228****	2.811 ± 0.435**	1.189 ± 0.240**
T	0.780 ± 0.161**	2.278 ± 0.300^{ns}	2.963 ± 0.275 *	0.960 ± 0.231*
O	1.554 ± 0.336****	3.780 ± 0.429****	2.493 ± 0.394**	1.170 ± 0.397*
C	12.883 ± 1.138****	34.685 ± 12.158***	2.642 ± 0.658 *	6.023 ± 1.697 ****

thymol and their biogenetic precursors *p*-cymene, γ-terpinene, which represent about 90% of both extracts, are the main compounds of these EOs.

Otherwise, cinnamon EO showed the most pronounced effect, both in terms of reducing photosynthetic activity and altering the algae morphology. Its main constituent, cinnamaldehyde, could interact more effectively with the cell membrane of the algae, inducing almost complete cell lysis compared to thymol and carvacrol. Otherwise, the antimicrobial activity of cinnamaldehyde has been extensively reviewed by Shreaz et al. (2016), who reported inhibition of cell wall biosynthesis and alteration of the cell membrane as its primary mode of action.

4. Conclusion

The integration of multiple analytical methods provided a comprehensive evaluation of the efficacy and impact of thyme, oregano and cinnamon EOs suspended in HG on microalgal biofilms isolated from the hypogeum of the Colosseum. While all EOs affected both cell morphology and biomolecule distributions, cinnamon EO exhibited the most pronounced effect, leading to extensive cell lysis. Notably, when encapsulated in HG, this oil was also the most effective in reducing photosynthetic activity over time, especially when applied for 48 h. These findings suggest the potential suitability of this treatment protocol for the conservation of stone cultural heritage. However, natural biofilm formation on stone surfaces is far more complex than in controlled laboratory conditions, as microbial communities interact positively and can adapt to extreme environmental conditions. For these reasons, while the promising results of this study provide an important foundation, further *in situ* investigation under real conditions are essential to validate the long-term effectiveness of this approach.

CRediT authorship contribution statement

Roberta Ranaldi: Conceptualization, Data curation, Formal analysis, Investigation, Validation, Visualization, Writing – original draft, Writing – review & editing. **Francesco Gabriele:** Conceptualization, Data curation, Investigation, Visualization, Writing – original draft, Writing – review & editing, Validation. **Lorenza Rugnini:** Conceptualization, Data curation, Formal analysis, Funding acquisition, Investigation, Project administration, Supervision, Validation, Visualization, Writing – original draft, Writing – review & editing. **Patrick Di Martino:** Funding acquisition, Supervision, Validation, Visualization, Writing – original draft, Writing – review & editing. **Rémy Agniel:** Data curation, Investigation, Writing – review & editing. **Francesco Scuderi:** Formal analysis, Validation, Writing – review & editing. **Roberto Braglia:** Conceptualization, Formal analysis, Funding acquisition, Project administration, Supervision, Validation, Writing – review & editing. **Antonella Canini:** Conceptualization, Formal analysis, Funding acquisition, Project administration, Supervision, Writing – review & editing. **Nicoletta Spreti:** Conceptualization, Funding acquisition, Project administration, Supervision, Writing – original draft, Writing – review & editing.

Funding

This publication was produced during the PhD program, XXXVIII cycle, in Evolutionary Biology and Ecology at the Tor Vergata University of Rome, with the support of a scholarship funded by D.M. No. 351 of April 9, 2022, under the PNRR-funded by the European Union-NextGenerationEU. We also acknowledged the Italian Ministry of Education, Universities and Research (Project Smart Cities and Communities and Social Innovation on Cultural Heritage - SCN_00520) for its financial support.

Declaration of competing interest

The authors declare that they have no known competing financial interests or personal relationships that could have appeared to influence the work reported in this paper.

Acknowledgments

We are grateful to the “Parco archeologico del Colosseo” for granting us the opportunity to sample and study microorganisms from the Colosseum hypogeum, an extraordinary site of inestimable cultural value. We also extend our thanks to the PhD program in Evolutionary Biology and Ecology at Tor Vergata University of Rome. Furthermore, we sincerely thank the Île-de-France Region for supporting the acquisition of scanning electron microscopy images through the SESAME system at the Microscopies & Analyses platform (CY Cergy Paris Université).

Appendix A. Supplementary data

Supplementary data to this article can be found online at https://doi.org/10.1016/j.ibiod.2025.106128.

Data availability

Data will be made available on request.

References

Andrade-Ochoa, S., Chacón-Vargas, K.F., Sánchez-Torres, L.E., Rivera-Chavira, B.E., Nogueda-Torres, B., Nevárez-Moorillón, G.V., 2021. Differential antimicrobial effect of essential oils and their main components: insights based on the cell membrane and external structure. Membranes 11, 405. https://doi.org/10.3390/membranes11060405.

Argyri, A.A., Doulgeraki, A.I., Varla, E.G., Bikouli, V.C., Natskoulis, P.I., Haroutounian, S. A., Moulas, G.A., Tassou, C.C., Chorianopoulos, N.G., 2021. Evaluation of plant origin essential oils as herbal biocides for the protection of caves belonging to natural and cultural heritage sites. Microorganisms 9, 1836. https://doi.org/10.3390/microorganisms9091836.

Avdanina, D.A., Zhgun, A.A., 2024. Rainbow code of biodeterioration to cultural heritage objects. Herit. Sci. 12, 187. https://doi.org/10.1186/s40494-024-01298-y.

Baglioni, P., Berti, D., Bonini, M., Carretti, E., Dei, L., Fratini, E., Giorgi, R., 2014. Micelle, microemulsions, and gels for the conservation of cultural heritage. Adv. Colloid Interface Sci. 205, 361–371. https://doi.org/10.1016/j.cis.2013.09.008.

Bartoli, F., Corradi, L., Hosseini, Z., Privitera, A., Zuena, M., Kumbaric, A., Graziani, V., Tortora, L., Sodo, A., Caneva, G., 2024. In vitro viability tests of new ecofriendly nanosystems incorporating essential oils for long-lasting conservation of stone artworks. Gels 10, 132. https://doi.org/10.3390/gels10020132.

Beć, K.B., Grabska, J., Huck, C.W., 2020. Biomolecular and bioanalytical applications of infrared spectroscopy - a review. Anal. Chim. Acta 1133, 150e177. https://doi.org/10.1016/j.aca.2020.04.015.

Berti, L., Villa, F., Toniolo, L., Cappitelli, F., Goidanich, S., 2024. Methodological challenges for the investigation of the dual role of biofilms on outdoor heritage. Sci. Total Environ. 954, 1764500. https://doi.org/10.1016/j.scitotenv.2024.176450.

Bontemps, Z., Hugoni, M., Moënne-Loccoz, Y., 2024. Ecological impact of mechanical cleaning method to curb black stain alterations on Paleolithic cave walls. Int. Biodeterior. Biodegrad. 191, 105797. https://doi.org/10.1016/j.ibiod.2024.105797.

Chelazzi, D., Giorgi, R., Baglioni, P., 2018. Microemulsions, micelles, and functional gels: how colloids and soft matter preserve works of art. Angew. Chem. Int. Ed. 57, 7296–7303. https://doi.org/10.1002/anie.201710711.

Chelu, M., 2024. Hydrogels with essential oils: recent advances in designs and applications. Gels 10, 636. https://doi.org/10.3390/gels10100636.

Chen, X., Liu, P., Luo, X., Huang, S., Wang, G., 2024. Study on the antibacterial activity and mechanism of cinnamaldehyde against methicillin-resistant *Staphylococcus aureus*. Eur. Food Res. Technol. 250, 1069–1081. https://doi.org/10.1007/s00217-023-04446-z.

Cirone, M., Figoli, A., Galiano, F., La Russa, M.F., Macchia, A., Mancuso, R., Ricca, M., Rovella, N., Taverniti, M., Ruffolo, S.A., 2023. Innovative methodologies for the conservation of cultural heritage against biodeterioration: a review. Coatings 13, 1986. https://doi.org/10.3390/coatings13121986.

Cuzman, O.A., Camaiti, M., Sacchi, B., Tiano, P., 2011. Natural antibiofouling agents as new control method for phototrophic biofilms dwelling on monumental stone surfaces. Int. J. Conserv. Sci. 2, 3–16.

De Leo, F., Dominguez-Moñino, I., Jurado, V., Bruno, L., Saiz-Jimenez, C., Urzì, C., 2022. Fungal outbreak in the Catacombs of SS. Marcellino and Pietro Rome (Italy): from diagnosis to an emergency treatment. Front. Microbiol. 13, 982933. https://doi.org/10.3389/fmicb.2022.982933.

de Sousa, D.P., Damasceno, R.O.S., Amorati, R., Elshabrawy, H.A., de Castro, R.D., Bezerra, D.P., Nunes, V.R.V., Gomes, R.C., Lima, T.C., 2023. Essential oils: chemistry and pharmacological activities. Biomolecules 13, 1144. https://doi.org/10.3390/biom13071144.

Di Vito, M., Vergari, L., Mariotti, M., Proto, M.R., Barbanti, L., Garzoli, S., Sanguinetti, M., Sabatini, L., Peduzzi, A., Bellardi, M.G., Mattarelli, P., Bugli, F., De Luca, D., 2022. Anti-mold effectiveness of a green emulsion based on *Citrus aurantium* hydrolate and *Cinnamomum zeylanicum* essential oil for the modern paintings restoration. Microorganisms 10, 205. https://doi.org/10.3390/microorganisms10020205.

Dutta, A., Chakraborty, A., 2018. Cinnamon in anticancer armamentarium: a molecular approach. J. Toxicol. 29, 8978731. https://doi.org/10.1155/2018/8978731.

Gabriele, F., Ranaldi, R., Bruno, L., Casieri, C., Rugnini, L., Spreti, N., 2023. Biodeterioration of stone monuments: studies on the influence of bioreceptivity on cyanobacterial biofilm growth and on the biocidal efficacy of essential oils in natural hydrogel. Sci. Total Environ. 870, 161901. https://doi.org/10.1016/j.scitotenv.2023.161901.

Gagliano Candela, R., Maggi, F., Lazzara, G., Rosselli, S., Bruno, M., 2019. The essential oil of *Thymbra capitata* and its application as a biocide on stone and derived surfaces. Plants 8, 300. https://doi.org/10.3390/plants8090300.

Genova, C., Fuentes, E., Sanmartín, P., Favero, G., Prieto, B., 2020. Phytochemical compounds as cleaning agents on granite colonized by phototrophic subaerial biofilms. Coatings 10, 295. https://doi.org/10.3390/coatings10030295.

Genova, C., Fuentes, E., Favero, G., Prieto, B., 2023. Evaluation of the cleaning effect of natural-based biocides: application on different phototropic biofilms colonizing the same granite wall. Coatings 13, 520. https://doi.org/10.3390/coatings13030520.

Gómez de Saravia, S.G., Silvia, E., Rastelli, S.E., Blustein, G., Viera, M.R., 2018. Natural compounds as potential algaecides for waterborne paints. J. Coating Technol. Res. 15, 1191–1200. https://doi.org/10.1007/s11998-018-0099-7.

Gu, J.D., 2024. Further research on essential oils. Int. Biodeterior. Biodegrad. 190, 105788. https://doi.org/10.1016/j.ibiod.2024.105788.

Hou, T., Sana, S.S., Li, H., Xing, Y., Nanda, A., Netala, V.R., Zhang, Z., 2022. Essential oils and its antibacterial, antifungal and anti-oxidant activity applications: a review. Food Biosci. 47, 101716. https://doi.org/10.1016/j.fbio.2022.101716.

Lee, H.J., Chung, Y.J., 2023. Antifungal, antibacterial, and interference effects of plant-extracted essential oils used for mural conservation at Buyeo Royal Tomb No. 1. Appl. Sci. 13, 3645. https://doi.org/10.3390/app13063645.

Liu, X., Koestler, R.J., Warscheid, T., Katayama, Y., Gu, J.D., 2020. Microbial deterioration and sustainable conservation of stone monuments and buildings. Nat. Sustain. 3, 991–1004. https://doi.org/10.1038/s41893-020-00602-5.

Long, M., Xiong, K., Lin, J., Tang, B., Ao, Z., Chen, Y., Xu, Z., 2024. Evaluation of ten plant-derived biocides for the inhibition of photosynthetic organisms on the karst surfaces of heritage building. Herit. Sci. 12, 344. https://doi.org/10.1186/s40494-024-01410-2.

Méndez, A., Sanmartín, P., Balboa, S., Trueba-Santiso, A., 2024. Environmental proteomics elucidates phototrophic biofilm responses to ornamental lighting on stone-built heritage. Microb. Ecol. 87, 147. https://doi.org/10.1007/s00248-024-02465-1.

Minotti, D., Vergari, L., Proto, M.R., Barbanti, L., Garzoli, S., Bugli, F., Sanguinetti, M., Sabatini, L., Peduzzi, A., Rosato, R., Bellardi, M.G., Mattarelli, P., De Luca, D., Di Vito, M., 2022. Il Silenzio: the first renaissance oil painting on canvas from the Uffizi Museum restored with a safe, green antimicrobial emulsion based on *Citrus aurantium* var. *amara* hydrolate and *Cinnamomum zeylanicum* essential oil. J. Fungi 8, 140. https://doi.org/10.3390/jof8020140.

Nabavi, S.F., Di Lorenzo, A., Izadi, M., Sobarzo-Sánchez, E., Daglia, M., Nabavi, S.M., 2015. Antibacterial effects of cinnamon: from farm to food, cosmetic and pharmaceutical industries. Nutrients 7, 7729–7748. https://doi.org/10.3390/nu7095359.

Paolino, B., Sorrentino, M.C., Pacifico, S., 2024. Greener solutions for biodeterioration of organic-media cultural heritage: where are we? Herit. Sci. 12, 334. https://doi.org/10.1186/s40494-024-01442-8.

Permadi, N., Nurzaman, M., Doni, F., Julaeha, E., 2024. Elucidation of the composition, antioxidant, and antimicrobial properties of essential oil and extract from *Citrus aurantifolia* (Christm.) Swingle peel. Saudi J. Biol. Sci. 31, 103987. https://doi.org/10.1016/j.sjbs.2024.103987.

Ranaldi, R., Rugnini, L., Gabriele, F., Spreti, N., Casieri, C., Di Marco, G., Gismondi, A., Bruno, L., 2022. Plant essential oils suspended into hydrogel: development of an easy-to-use protocol for the restoration of stone cultural heritage. Int. Biodeterior. Biodegrad. 172, 105436. https://doi.org/10.1016/j.ibiod.2022.105436.

Ranaldi, R., Rugnini, L., Migliore, G., Tasso, F., Gabriele, F., Spreti, N., Scuderi, F., Braglia, R., Di Martino, P., Pujia, A., Canini, A., 2025. The role of essential oils as eco-friendly strategy to control biofilm collected in the Colosseum (Rome, Italy). Appl. Microbiol. Biotechnol. 109, 48. https://doi.org/10.1007/s00253-025-13433-1.

Reale, R., Medeghini, L., Botticelli, M., 2024. Stealing from phytotherapy-heritage conservation with essential oils: a review, from remedy to sustainable restoration product. Sustainability 16, 5110. https://doi.org/10.3390/su16125110.

Rippka, R., Deruelles, J., Waterbury, J.B., Herdman, M., Stainer, R.Y., 1979. Generic assignments, strain histories and properties of pure cultures of cyanobacteria. J. Gen. Microbiol. 111, 1–61. https://doi.org/10.1099/00221287-111-1-1.

Romani, M., Warscheid, T., Nicole, L., Marcon, L., Di Martino, P., Suzuki, M.T., Lebaron, P., Lami, R., 2022. Current and future chemical treatments to fight biodeterioration of outdoor building materials and associated biofilms: moving away from ecotoxic and towards efficient, sustainable solutions. Sci. Total Environ. 802, 149846. https://doi.org/10.1016/j.scitotenv.2021.149846.

Rugnini, L., Migliore, G., Tasso, F., Ellwood, N.T.W., Sprocati, A.R., Bruno, L., 2020. Biocidal activity of phyto-derivative products used on phototrophic biofilms growing on stone surfaces of the Domus Aurea in Rome (Italy). Appl. Sci. 10, 6584. https://doi.org/10.3390/app10186584.

Russo, R., Palla, F., 2023. Plant essential oils as biocides in sustainable strategies for the conservation of cultural heritage. Sustainability 15, 8522. https://doi.org/10.3390/su15118522.

Sanmartín, P., Bosch-Roig, P., Pangallo, D., Kraková, L., Serrano, M., 2023. Unraveling disparate roles of organisms, from plants to bacteria, and viruses on built cultural heritage. Appl. Microbiol. Biotechnol. 107, 2027–2037. https://doi.org/10.1007/s00253-023-12423-5.

Shreaz, S., Wani, W.A., Behbehani, J.M., Raja, V., Irshad, M., Karched, M., Ali, I., Siddiqi, W.A., Hun, L.T., 2016. Cinnamaldehyde and its derivatives, a novel class of antifungal agents. Fitoterapia 112, 116–131. https://doi.org/10.1016/j.fitote.2016.05.016.

Spada, M., Sorella, F., Galeotti, M., Tosini, I., Cuzman, O.A., 2021. Non-invasive technologies to timely screen out different application conditions of essential oils on stone. Int. Biodeterior. Biodegrad. 163, 105285. https://doi.org/10.1016/j.ibiod.2021.105285.

Stanaszek-Tomal, E., 2020. Environmental factors causing the development of microorganisms on the surfaces of national cultural monuments made of mineral building materials - review. Coatings 10, 1203. https://doi.org/10.3390/coatings10121203.

Wang, L., Huang, J., Sanmartín, P., Di Martino, P., Wu, F., Urzì, C.E., Gu, J.-D., Liu, X., 2025. Water determines geomicrobiological impact on stone heritage. Nat. Geosci. 18, 108–111. https://doi.org/10.1038/s41561-024-01631-x.

Xie, X., Cong, W., Zhao, F., Li, H., Xin, W., Hou, G., Wang, C., 2018. Synthesis, physiochemical property and antimicrobial activity of novel quaternary ammonium salts. J. Enzym. Inhib. Med. Chem. 33, 98–105. https://doi.org/10.1080/14756366.2017.1396456.

Xin, X., Huang, G., Liu, X., An, C., Yao, Y., Weger, H., Zhang, P., Chen, X., 2017. Molecular toxicity of triclosan and carbamazepine to green algae *Chlorococcum* sp.: a single cell view using synchrotron-based Fourier transform infrared

spectromicroscopy. Environ. Pollut. 226, 12–20. https://doi.org/10.1016/j.envpol.2017.04.00702.

Xiong, Q., Hu, L.X., Liu, Y.S., Wang, T.T., Ying, G.G., 2019. New insight into the toxic effects of chloramphenicol and roxithromycin to algae using FTIR spectroscopy. Aquat. Toxicol. 207, 197–207. https://doi.org/10.1016/j.aquatox.2018.12.017.

Zhang, J., Cheng, L., Li, H., Chen, X., Zhang, L., Shan, T., Wang, J., Chen, D., Shen, J., Zhou, X., Gou, L., Zhang, L., Zhou, X., Ren, B., 2025. Challenges of quaternary ammonium antimicrobial agents: mechanisms, resistance, persistence and impacts on the microecology. Sci. Total Environ. 958, 178020. https://doi.org/10.1016/j.scitotenv.2024.178020.